

Article

McCARD Criticality Benchmark Analyses with Various Evaluated Nuclear Data Libraries

Ho Jin Park ¹, Mohammad Alosaimi ², Seong-Ah Yang ¹, Heejeong Jeong ³ and Sung Hoon Choi ^{3,*}¹ Department of Nuclear Engineering, Kyung Hee University, Yongin 17104, Korea² King Abdullah City for Atomic and Renewable Energy, Riyadh 12244, Saudi Arabia³ Korea Atomic Energy Research Institute, Daejeon 34057, Korea

* Correspondence: cshoon@kaeri.re.kr; Tel.: +82-42-868-8642

Abstract: International Criticality Safety Benchmark Evaluation Project (ICSBEP) criticality analyses were conducted using the McCARD Monte Carlo code for 85 selected benchmark problems with 7 evaluated nuclear data libraries (ENDLs): ENDF/B-VII.1, ENDF/B-VIII.0, JENDL-4.0, JENDL-5.0, JEFF-3.3, TENDL-2021, and CENDL-3.2. Regarding the analyses, it was confirmed that the k_{eff} results are sensitive to the ENDL. It is noted that the new-version ENDLs show better performance in the fast benchmark cases, while on the other hand, there are no significant differences in k_{eff} among the different ENDLs in the thermal benchmark cases. The sensitivity of the k_{eff} results depending on the ENDL may impact nuclear core design parameters such as the shutdown margin, critical boron concentration, and power defects. This study and k_{eff} results will be a good reference in the development of new types of nuclear cores or new design codes.

Keywords: Monte Carlo; McCARD; criticality analysis; ICSBEP; ENDF/B-VIII.0; ENDF/B-VII.1; JENDL-4.0; JENDL-5.0; TENDL-2021; CENDL-3.2; JEFF-3.3



Citation: Park, H.J.; Alosaimi, M.; Yang, S.-A.; Jeong, H.; Choi, S.H. McCARD Criticality Benchmark Analyses with Various Evaluated Nuclear Data Libraries. *Energies* **2022**, *15*, 6852. <https://doi.org/10.3390/en15186852>

Academic Editors: Marcin Kamiński and Mateus Mendes

Received: 3 September 2022

Accepted: 14 September 2022

Published: 19 September 2022

Publisher's Note: MDPI stays neutral with regard to jurisdictional claims in published maps and institutional affiliations.



Copyright: © 2022 by the authors. Licensee MDPI, Basel, Switzerland. This article is an open access article distributed under the terms and conditions of the Creative Commons Attribution (CC BY) license (<https://creativecommons.org/licenses/by/4.0/>).

1. Introduction

In various nuclear engineering applications, atomic and nuclear data are widely used as important and critical inputs to solve particle transport balance equations. Many research institutes have provided the nuclear data as evaluated nuclear data libraries (ENDLs) in a traditional ENDF-6 (evaluated nuclear data file) format, which are processed from measurements, compilations, and evaluations. The ENDF-6 format includes general information, resonance parameter data, reaction cross section, angular distribution, and their covariance data. The Cross Section Evaluation Working Group, organized by the United States (i.e., Brookhaven, Oak Ridge, and Argonne national Laboratories) and international nuclear societies, has released ENDF/B ENDLs. Among the versions in this series, ENDF/B-VII.1 [1] is widely used in particle transport simulation codes for nuclear reactor physics and core design analysis. An up-to-date version ENDF/B-VIII.0 [2], was released in February 2018. This version includes new evaluation data of the six nuclides (i.e., ^1H , ^{16}O , ^{56}Fe , ^{235}U , ^{238}U , ^{239}Pu) from the CIELO (Collaborative International Evaluation Library Organization) project. At the time of release, the neutron-reaction evaluation data for 557 materials in ENDF/B-VIII.0 were totally new or partially updated, including improved thermal neutron scattering data. Meanwhile, the Japan Atomic Energy Research Institute and Japanese Nuclear Data Committee (JNDC) have been continuously providing a series of Japanese Evaluated Nuclear Data Libraries (JENDLs), including JENDL-4.0 [3] released in May 2010 and an up-to-date version JENDL-5.0 [4] released in December 2021. In JENDL-5.0, the number of neutron sub-libraries was increased from 406 to 795 and the energy region was extended from 20 MeV to 200 MeV. Otherwise, the OECD (Organization for Economic Cooperation and Development)/NEA (Nuclear Energy Agency) Data Bank has coordinated the Joint Evaluated Fission and Fusion (JEFF) ENDL development for the last 35 years. Released in November 2017 JEFF-3.3 [5] provided 562 evaluations for neutron reactions. In

another example, the Paul Scherrer Institute (PSI) and International Atomic Energy Agency nuclear data section developed a series of TENDL ENDLs. TENDL [6] provides the outputs of the TALYS code [7] to analyze and predict nuclear reactions. The latest version, TENDL-2021, provides 2813 evaluations for neutron reactions while ENDF/B-VIII.0 has 557 isotopic data files. And as a final example, the China Nuclear Data Center has released a series of Chinese general purpose Evaluated Nuclear Data Library (CENDL). CENDL-3.2 [8] is the latest release of CENDL, which has ENDF-6 formatted neutron reactions for 272 isotopes.

As stated above, a variety of ENDLs have been released and continuously updated by their providers around the world for use in various nuclear physics research and applications. To validate the newly developed ENDLs, the integral testing work has been performed using various benchmark problems. The International Criticality Safety Benchmark Evaluation Project (ICSBEP) [9] is one of the representative integral testing programs from critical experiments. The ICSBEP criticality analysis problems were classified by various fuel types and system spectrums. The ICSBEP handbook provides an overview of experiments, benchmark specifications, and some results for sample calculations by KENO-V in the SCALE code package [10], MCNP [11], and ONEDANT/TWODANT in the DANTSYS code package [12]. There are many studies and results for the ICSBEP benchmark problems with various ENDLs [13–16].

Recently, the Korea Atomic Energy Research Institute (KAERI) and King Abdullah City for Atomic and Renewable Energy (K.A.CARE) established the KAERI-K.A.CARE joint R&D center at KAERI to continue effective and close cooperation for the establishment of the National Nuclear Laboratory in Saudi Arabia. This center has carried out various joint R&D programs, an example of which is a project called “Application of a Monte-Carlo Neutron/Photon Transport Simulation Code for Advanced Shielding Design of Nuclear Reactors”. The main goal of this project is to train K.A.CARE engineers in a nuclear core shielding design analysis and to validate the McCARD [17] Monte Carlo (MC) code to be used for the advanced shielding design and analyses of new-type reactors. To validate the capability of the McCARD code for criticality analyses, KAERI and K.A.CARE engineers performed criticality analyses with the McCARD code and the up-to-date ENDLs.

In this study, seven ENDLs—ENDF/B-VII.1, ENDF/B-VIII.0, JENDL-4.0, JENDL-5.0, JEFF-3.3, TENDL-2021, and CENDL-3.2—were tested and examined by performing McCARD criticality analyses for selected ICSBEP benchmark problems. Section 2 briefly describes the configuration of the selected ICSBEP problems for criticality analysis and explains how to generate the continuous energy cross section from the raw ENDLs. Section 3 presents the results of the ICSBEP criticality analyses calculated by the McCARD MC code with the various ENDLs. The results are provided by categorizing the fuel fissile isotopes, fuel form, and system spectrum. A summary and conclusions are given in Section 4.

2. Evaluated Nuclear Data Libraries and ICSBEP Benchmarks for Criticality Analyses

2.1. Evaluated Nuclear Data Libraries

Various up-to-date evaluated nuclear data libraries are first prepared for the integral testing work via MC criticality analyses. First of all, the most up-to-date NJOY code [18] and its user inputs for all nuclides at three temperature points (300 K, 600 K, and 900 K) were prepared to process the raw ENDLs and to generate MC continuous energy cross section libraries in ACE format. Figure 1 shows the general flow chart of the ACE-formatted continuous-energy (CE) nuclear data library generation in the NJOY code. Neutron CE cross sections for each isotope are generated by the flow of the RECONR, BROADR, UNRESR, PURR, and ACER modules in NJOY, whereas the thermal scattering cross sections are generated by the RECONR, BROADR, LEAPR, THERMR, and ACER modules. The RECONR module reconstructs point-wise cross sections from ENDF resonance parameters and interpolation schemes, which are then processed into Doppler-broadens and thins point-wise cross sections by the BROADR module. The UNRESR and PURR modules generate effective self-shielded point-wise cross sections and probability tables in unresolved energy regions. For the thermal scattering cross section generation, LEAPR calculates the thermal

scattering law while THERMR produces cross sections and energy-to-matrices for free or bound scattering in the thermal energy range. Lastly, the ACER module prepares libraries in ACE format for a CE MC code (e.g., MCNP, McCARD, RMC).

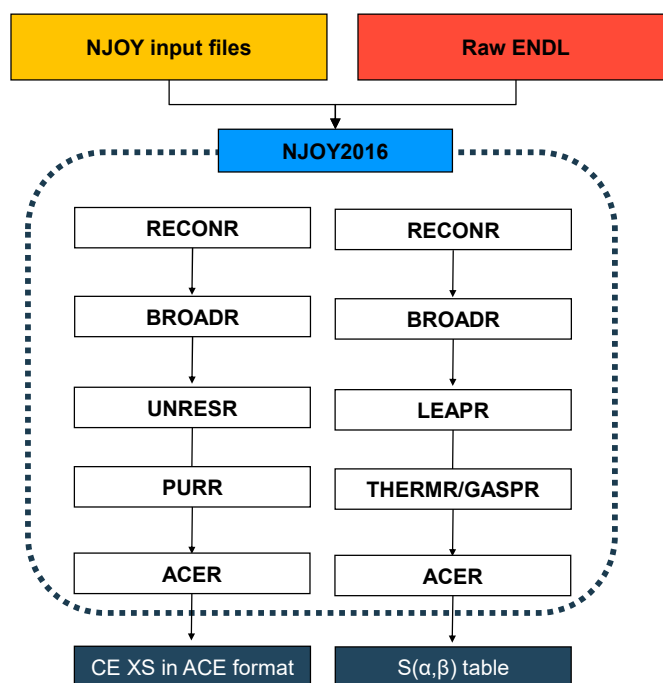


Figure 1. A flowchart of Monte Carlo CE library generation in NJOY code.

Table 1 summarizes the newly generated Monte Carlo CE cross section libraries. In this study, only the five most often used thermal scattering cross sections (i.e., H in H₂O, D in D₂O, Be metal, Be in BeO, and C in graphite) were generated for all ENDLs. As shown in Table 1, there is no thermal scattering cross section data in CENDL-3.2 and only one thermal scattering cross section data in TENDL-2021. Accordingly, the lack of thermal scattering cross section data was substituted by ENDF/B-VIII.0. In general, the ENDF/B cross section library has been used all around the world in various research and fields, and among the ENDF/B versions, ENDF/B-VIII.0 is the latest version. According to this, we used the thermal scattering cross section data for the lack of other ENDL thermal scattering cross section data.

Table 1. A summary of the generated Monte Carlo CE cross section libraries.

ENDL	Years of Release	Number of Generated CE Libraries/Total Number	
		Neutron	Thermal Scattering
ENDF/B-VII.1	2011	393/423	5/21
ENDF/B-VIII.0	2018	544/557	5/34
JENDL-4.0	2011	405/406	5/16
JENDL-5.0	2021	233/795	5/37
JEFF-3.3	2018	558/562	5/20
TENDL-2021 *	2021	630/2813	1/1
CENDL-3.2	2020	270/272	None

* CE neutron reaction library was taken from the official website.

2.2. Selected International Criticality Benchmark Problems

To perform the integral testing work for criticality capability, 85 benchmark problems were selected from the ICSBEP handbook [9]. The 85 ICSBEP benchmarks were selected from the well-known relevant experiments (i.e., godiva, jezebel, flattop) or the problems that have the results by MCNP with various ENDLs. In general, they boil down to three

criteria: fuel fissile isotope, fuel form, and system spectrum. Fuel fissile isotopes can be categorized into high-enriched uranium (HEU), low-enriched uranium (LEU), plutonium (PU), ^{233}U (U233), and mixed composition (MIX). Fuel forms are defined as metal (MET), compound (COMP), and solution (SOL), and system spectrum is classified as fast (FAST) and thermal (THERMAL). The ICSBEP handbook provides the identification (ID) for each benchmark problem as a combination of the fuel isotope, fuel form, and spectrum type.

Table 2 lists the 85 selected ICSBEP benchmark problems, providing benchmark IDs, categories, reference k_{eff} , and short IDs for the sake of convenient reference. The McCARD inputs for each ICSBEP benchmark problem were prepared. All the McCARD calculations were performed by employing 10,000 neutron particles per cycle with 1000 active cycles and 50 inactive cycles. The initial neutron sources were uniformly distributed in the system boundary for MC eigenvalue calculations. Figures 2 and 3 show the neutron energy spectra for five fast benchmarks (i.e., Jezebel, Jezebel-240, Godiva, Flattop-25, and Jezebel-233) and six thermal benchmarks (i.e., LCT001c1, LCT002c1, LCT006c1, ORNL-1, PNL-3, and ORNL-11), respectively. In the fast benchmarks, the energy spectra are similar to the energy distribution of neutrons from fission reactions. In the thermal benchmarks, the neutron energy spectra are attributed to neutron moderation or slowing-down. As shown in Table 2, the thermal scattering law (TSL) sub-library for light water was only used in this ICSBEP benchmark analyses.

Table 2. A list of selected International Criticality Safety Benchmark Problems.

No.	Short Name	Handbook ID	Category	Benchmark k_{eff}	Uncertainty of k_{eff}	TSL *
1	Jezebel	PU-MET-FAST-001	Pu Fast	1.0000	0.00200	-
2	Jezebel-240	PU-MET-FAST-002	Pu Fast	1.0000	0.00200	-
3	PMF-020	PU-MET-FAST-020	Pu Fast	0.9993	0.00170	-
4	PMF-022	PU-MET-FAST-022	Pu Fast	1.0000	0.00210	-
5	PMF-005	PU-MET-FAST-005	Pu Fast	1.0000	0.00130	-
6	PMF-006	PU-MET-FAST-006	Pu Fast	1.0000	0.00300	-
7	PMF-010	PU-MET-FAST-010	Pu Fast	1.0000	0.00180	-
8	PMF-011	PU-MET-FAST-011	Pu Fast	1.0000	0.00100	Light water
9	Godiva	HEU-MET-FAST-001	HEU Fast	1.0000	0.00100	-
10	Flattop-25	HEU-MET-FAST-028	HEU Fast	1.0000	0.00300	-
11	HMF-002 c2	HEU-MET-FAST-002 c2	HEU Fast	1.0000	0.00300	-
12	HMF-002 c3	HEU-MET-FAST-002 c3	HEU Fast	1.0000	0.00300	-
13	HMF-002 c4	HEU-MET-FAST-002 c4	HEU Fast	1.0000	0.00300	-
14	HMF-002 c5	HEU-MET-FAST-002 c5	HEU Fast	1.0000	0.00300	-
15	HMF-002 c6	HEU-MET-FAST-002 c6	HEU Fast	1.0000	0.00300	-
16	HMF-004	HEU-MET-FAST-004	HEU Fast	1.0020	-	-
17	HMF-018	HEU-MET-FAST-018	HEU Fast	1.0000	0.00140	-
18	HMF-027	HEU-MET-FAST-027	HEU Fast	1.0000	0.00250	-
19	HMF-032 c1	HEU-MET-FAST-032 c1	HEU Fast	1.0000	0.00130	-
20	HMF-032 c2	HEU-MET-FAST-032 c2	HEU Fast	1.0000	0.00260	-
21	HMF-032 c3	HEU-MET-FAST-032 c3	HEU Fast	1.0000	0.00130	-
22	HMF-032 c4	HEU-MET-FAST-032 c4	HEU Fast	1.0000	0.00130	-
23	Jezebel-233	U233-MET-FAST-001	U233 Fast	1.0000	0.00100	-
24	U233-MF003	U233-MET-FAST-003	U233 Fast	1.0000	0.00100	-
25	U233-MF004	U233-MET-FAST-004	U233 Fast	1.0000	0.00070	-
26	U233-MF005	U233-MET-FAST-005	U233 Fast	1.0000	0.00300	-
27	Flattop-23	U233-MET-FAST-006	U233 Fast	1.0000	0.00100	-
28	MMF-001	MIX-MET-FAST-001	MIX Fast	1.0000	0.00160	-
29	MMF-002 c1	MIX-MET-FAST-002 c1	MIX Fast	1.0000	0.00440	-
30	MMF-002 c2	MIX-MET-FAST-002 c2	MIX Fast	1.0000	0.00440	-
31	MMF-002 c3	MIX-MET-FAST-002 c3	MIX Fast	1.0000	0.00440	-
32	ORNL-1	HEU-SOL-THERM-013 c1	HEU Thermal	1.0012	0.00260	Light water

Table 2. Cont.

No.	Short Name	Handbook ID	Category	Benchmark k_{eff}	Uncertainty of k_{eff}	TSL *
33	ORNL-2	HEU-SOL-THERM-013 c2	HEU Thermal	1.0007	0.00360	Light water
34	ORNL-3	HEU-SOL-THERM-013 c3	HEU Thermal	1.0009	0.00360	Light water
35	ORNL-4	HEU-SOL-THERM-013 c4	HEU Thermal	1.0003	0.00360	Light water
36	ORNL-10	HEU-SOL-THERM-032	HEU Thermal	1.0015	0.00260	Light water
37	LCT-001 c1	LEU-COMP-THERM-001 c1	LEU Thermal	1.0000	0.00310	Light water
38	LCT-001 c2	LEU-COMP-THERM-001 c2	LEU Thermal	0.9998	0.00310	Light water
39	LCT-001 c3	LEU-COMP-THERM-001 c3	LEU Thermal	0.9998	0.00310	Light water
40	LCT-001 c4	LEU-COMP-THERM-001 c4	LEU Thermal	0.9998	0.00310	Light water
41	LCT-001 c5	LEU-COMP-THERM-001 c5	LEU Thermal	0.9998	0.00310	Light water
42	LCT-001 c6	LEU-COMP-THERM-001 c6	LEU Thermal	0.9998	0.00310	Light water
43	LCT-001 c7	LEU-COMP-THERM-001 c7	LEU Thermal	0.9998	0.00310	Light water
44	LCT-001 c8	LEU-COMP-THERM-001 c8	LEU Thermal	0.9998	0.00310	Light water
45	LCT-002 c1	LEU-COMP-THERM-002 c1	LEU Thermal	0.9997	0.00200	Light water
46	LCT-002 c2	LEU-COMP-THERM-002 c2	LEU Thermal	0.9997	0.00200	Light water
47	LCT-002 c3	LEU-COMP-THERM-002 c3	LEU Thermal	0.9997	0.00200	Light water
48	LCT-006 c1	LEU-COMP-THERM-006 c1	LEU Thermal	1.0000	0.00200	Light water
49	LCT-006 c2	LEU-COMP-THERM-006 c2	LEU Thermal	1.0000	0.00200	Light water
50	LCT-006 c3	LEU-COMP-THERM-006 c3	LEU Thermal	1.0000	0.00200	Light water
51	LCT-006 c4	LEU-COMP-THERM-006 c4	LEU Thermal	1.0000	0.00200	Light water
52	LCT-006 c5	LEU-COMP-THERM-006 c5	LEU Thermal	1.0000	0.00200	Light water
53	LCT-006 c6	LEU-COMP-THERM-006 c6	LEU Thermal	1.0000	0.00200	Light water
54	LCT-006 c7	LEU-COMP-THERM-006 c7	LEU Thermal	1.0000	0.00200	Light water
55	LCT-006 c8	LEU-COMP-THERM-006 c8	LEU Thermal	1.0000	0.00200	Light water
56	LCT-006 c9	LEU-COMP-THERM-006 c9	LEU Thermal	1.0000	0.00200	Light water
57	LCT-006 c10	LEU-COMP-THERM-006 c10	LEU Thermal	1.0000	0.00200	Light water
58	LCT-006 c11	LEU-COMP-THERM-006 c11	LEU Thermal	1.0000	0.00200	Light water
59	LCT-006 c12	LEU-COMP-THERM-006 c12	LEU Thermal	1.0000	0.00200	Light water
60	LCT-006 c13	LEU-COMP-THERM-006 c13	LEU Thermal	1.0000	0.00200	Light water
61	LCT-006 c14	LEU-COMP-THERM-006 c14	LEU Thermal	1.0000	0.00200	Light water
62	LCT-006 c15	LEU-COMP-THERM-006 c15	LEU Thermal	1.0000	0.00200	Light water
63	LCT-006 c16	LEU-COMP-THERM-006 c16	LEU Thermal	1.0000	0.00200	Light water
64	LCT-006 c17	LEU-COMP-THERM-006 c17	LEU Thermal	1.0000	0.00200	Light water
65	LCT-006 c18	LEU-COMP-THERM-006 c18	LEU Thermal	1.0000	0.00200	Light water
66	LCT-010 c9	LEU-COMP-THERM-010 c9	LEU Thermal	1.0000	0.00280	Light water
67	LCT-010 c11	LEU-COMP-THERM-010 c11	LEU Thermal	1.0000	0.00280	Light water
68	LCT-010 c12	LEU-COMP-THERM-010 c12	LEU Thermal	1.0000	0.00280	Light water
69	LCT-010 c14	LEU-COMP-THERM-010 c14	LEU Thermal	1.0000	0.00280	Light water
70	LCT-010 c15	LEU-COMP-THERM-010 c15	LEU Thermal	1.0000	0.00280	Light water
71	LCT-010 c16	LEU-COMP-THERM-010 c16	LEU Thermal	1.0000	0.00280	Light water
72	LCT-010 c17	LEU-COMP-THERM-010 c17	LEU Thermal	1.0000	0.00280	Light water
73	LCT-010 c18	LEU-COMP-THERM-010 c18	LEU Thermal	1.0000	0.00280	Light water
74	LCT-017 c13	LEU-COMP-THERM-017 c13	LEU Thermal	1.0000	0.00310	Light water
75	LCT-017 c15	LEU-COMP-THERM-017 c15	LEU Thermal	1.0000	0.00310	Light water
76	LCT-017 c18	LEU-COMP-THERM-017 c18	LEU Thermal	1.0000	0.00310	Light water
77	LCT-017 c21	LEU-COMP-THERM-017 c21	LEU Thermal	1.0000	0.00310	Light water
78	IPEN/MB-01	LEU-COMP-THERM-077	LEU Thermal	1.0003	0.00100	Light water
79	LMT-007 c1	LEU-MET-THERM-007 c1	LEU Thermal	0.9983	0.01140	Light water
80	LMT-007 c2	LEU-MET-THERM-007 c2	LEU Thermal	0.9976	0.00680	Light water
81	PNL-3	PU-SOL-THERM-011 c18-1	Pu Thermal	1.0000	0.00520	Light water
82	PNL-4	PU-SOL-THERM-011 c18-6	Pu Thermal	1.0000	0.00520	Light water
83	PNL-5	PU-SOL-THERM-011 c16-5	Pu Thermal	1.0000	0.00520	Light water
84	PST011c16-1	PU-SOL-THERM-011 c16-1	Pu Thermal	1.0000	0.00520	Light water
85	ORNL-11	U233-SOL-THERM-008	U233 Thermal	1.0006	0.00290	Light water

* TSL is a thermal scattering law sub-library.

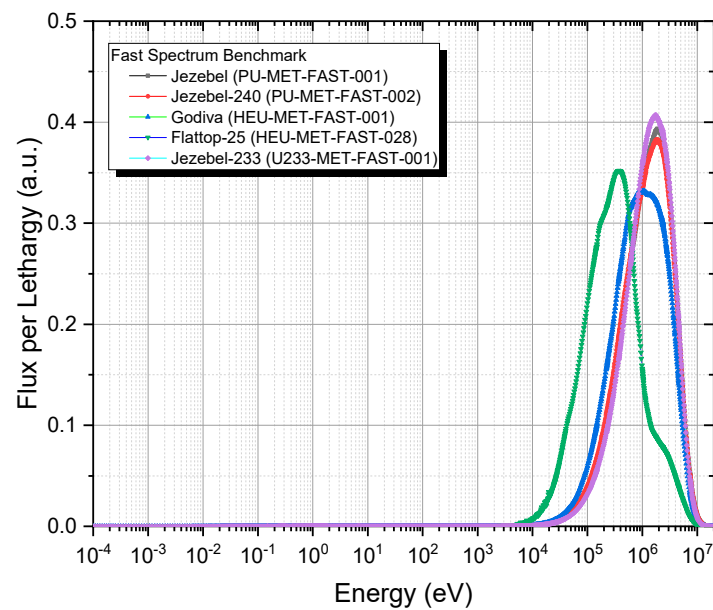


Figure 2. Spectra of example fast benchmark problems.

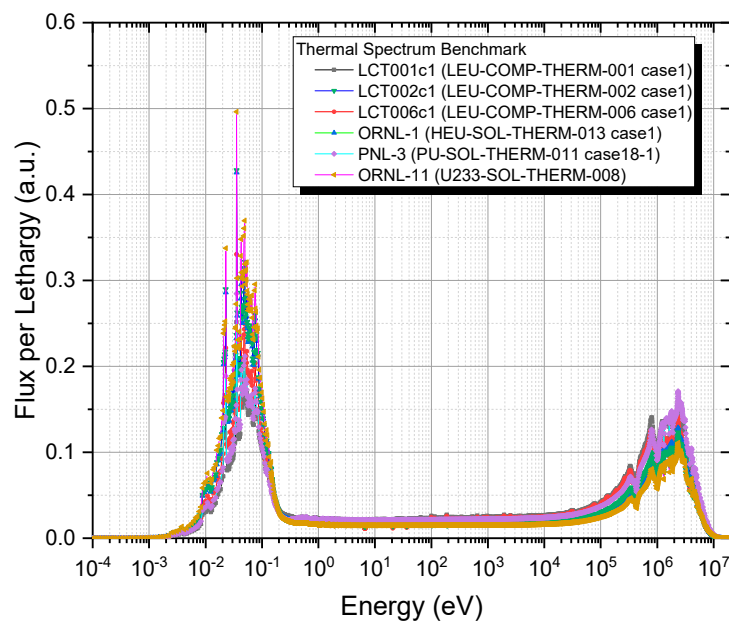


Figure 3. Spectra of example thermal benchmark problems.

3. ICSBEP Criticality Benchmark Analyses by McCARD

3.1. Fast Criticality Benchmarks

Table 3 shows the k_{eff} values calculated by McCARD with the seven ENDLs (ENDF/B-VII.1, ENDF/B-VIII.0, JENDL-4.0, JENDL-5.0, JEFF-3.3, TENDL-2021, and CENDI-3.2). Figure 4 plots the difference ($\Delta\rho_{cal}$) between the calculated and experimental k_{eff} for the 31 fast benchmark problems calculated by

$$\Delta\rho_{cal} = \frac{k_{cal}^i - k_{exp}^i}{k_{cal}^i \cdot k_{exp}^i} \cdot 10^5. \quad (1)$$

Table 3. k_{eff} values for the fast benchmarks with the different evaluated nuclear data libraries.

No.	Short Name	k_{eff} (McCARD) *						
		ENDF/B-VII.1	ENDF/B-VIII.0	JENDL-4.0	JENDL-5.0	JEFF-3.3	TENDL-2021	CENDL-3.2
1	Jezebel	1.00021	0.99995	0.99837	0.99925	0.99951	1.00004	1.00193
2	Jezebel-240	1.00041	1.00160	0.99849	0.99870	1.00151	1.00361	1.00271
3	PMF-020	0.99836	0.99697	0.99551	0.99826	0.99955	1.00023	0.99714
4	PMF-022	0.99870	0.99815	0.99694	0.99816	0.99800	0.99856	1.00034
5	PMF-005	1.00078	0.99944	1.00184	0.99890	1.00135	0.99663	1.00127
6	PMF-006	1.00140	1.00011	0.99906	1.00195	1.00366	1.00396	0.99946
7	PMF-010	0.99986	0.99799	0.99720	0.99972	1.00047	1.00095	0.99876
8	PMF-011	1.00041	1.00066	1.00194	1.00072	1.00108	1.00024	1.00222
9	Godiva	0.99991	1.00014	0.99760	0.99925	1.00005	1.00074	0.99974
10	Flattop-25	1.00299	1.00107	0.99812	1.00081	1.00433	1.00544	1.00184
11	HMF-002 c2	1.00248	1.00031	0.99762	1.00066	1.00381	1.00493	1.00073
12	HMF-002 c3	1.00063	0.99877	0.99593	0.99881	1.00206	1.00340	0.99918
13	HMF-002 c4	0.99990	0.99780	0.99497	0.99808	1.00118	1.00208	0.99782
14	HMF-002 c5	1.00021	0.99812	0.99520	0.99845	1.00162	1.00268	0.99882
15	HMF-002 c6	1.00160	0.99957	0.99677	0.99970	1.00294	1.00372	0.99983
16	HMF-004	1.00296	1.00189	1.00378	1.00223	1.00236	1.00139	1.00463
17	HMF-018	1.00006	1.00007	0.99764	0.99882	1.00032	1.00096	1.00044
18	HMF-027	1.00074	1.00046	1.00156	1.00323	1.00445	1.00134	1.00297
19	HMF-032 c1	1.00415	1.00183	0.99897	1.00233	1.00509	1.00567	1.00301
20	HMF-032 c2	1.00476	1.00246	0.99953	1.00296	1.00548	1.00652	1.00335
21	HMF-032 c3	1.00022	0.99821	0.99579	0.99862	1.00082	1.00148	0.99967
22	HMF-032 c4	1.00070	0.99973	0.99754	0.99973	1.00136	1.00220	1.00029
23	Jezebel-233	0.99974	1.00029	0.99906	0.99978	1.00084	1.00102	1.00112
24	U233-MF003	0.99917	0.99951	0.99861	1.00035	1.00144	1.00138	1.00038
25	U233-MF004	0.99835	0.99939	1.00012	0.99710	1.00000	0.99672	0.99966
26	U233-MF005	0.99578	0.99719	0.99590	0.99647	0.99709	0.99670	0.99555
27	Flattop-23	0.99888	0.99998	0.99849	1.00043	1.00352	1.00322	0.99900
28	MMF-001	0.99961	0.99949	0.99788	0.99895	0.99899	0.99934	0.99885
29	MMF-002 c1	1.00543	1.00375	1.00166	1.00421	1.00673	1.00714	1.00376
30	MMF-002 c2	1.00573	1.00393	1.00172	1.00419	1.00688	1.00731	1.00415
31	MMF-002 c3	1.00577	1.00447	1.00173	1.00391	1.00723	1.00861	1.00340

* The statistical uncertainties of the calculated k_{eff} are less than 10 pcm.

Here, k_{exp} and k_{cal} are the experimental and calculated k_{eff} for the i -th benchmark problem, respectively. The statistical uncertainties of the calculated k_{eff} are less than 10 pcm. Accordingly, error bars of the calculated k_{eff} are not marked in Figure 4 because they are relatively small compared to the uncertainties of the reference k_{eff} values. Overall, the values from JENDL-4.0 are lower than those from the other ENDLs whereas JEFF-3.3 and TENDL-2021 have higher values than the other ENDLs. For statistical analyses, root mean square (RMS) error and chi square (χ^2) can be utilized as indicators to confirm the differences between the experimental and calculated k_{eff} . Typically, RMS error and chi square values can be calculated by

$$RMS\ error(\%) = \sqrt{\frac{1}{N} \sum_{i=1}^N (k_{cal}^i - k_{exp}^i)^2}, \quad (2)$$

$$\chi^2 = \frac{1}{N} \sum_{i=1}^N \left(\frac{k_{cal}^i - k_{exp}^i}{\sigma_{exp}^i} \right)^2. \quad (3)$$

where σ_{exp} is the uncertainty of k_{exp} provided from each benchmark document [9]. The number of benchmark problems is N .

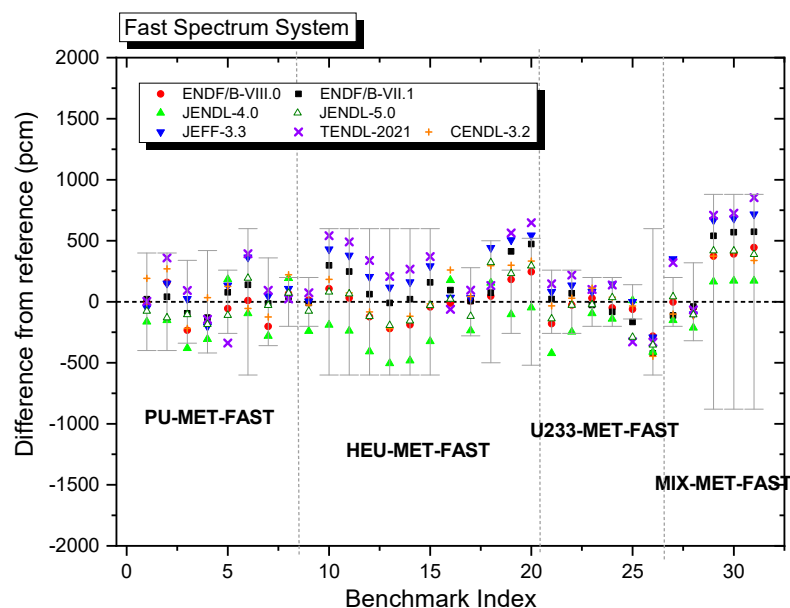


Figure 4. The difference between calculated and experimental k_{eff} by ENDL for the ICSBEP fast benchmarks.

Table 4 shows the RMS errors and chi square values for the 31 fast benchmark problems. It is observed that the new version ENDLs show better performance than the old versions in the fast benchmarks. The RMS error of ENDF/B-VII.1 is 244 pcm, whereas that of ENDF/B-VIII.0 is 179 pcm. The RMS error of JENDL-4.0 is 258 pcm compared to that of JENDL-5.0 at 199 pcm. It is noted that ENDF/B-VIII.0 has the smallest RMS error and chi square value among the ENDLs. In the 31 fast benchmarks, the average uncertainty of k_{exp} is about 220 pcm.

Table 4. RMS errors and chi square values of the 31 fast benchmarks for different evaluated nuclear data libraries.

ENDL	RMS Error (pcm)	χ^2
ENDF/B-VII.1	244	1.02
ENDF/B-VIII.0	179	0.72
JENDL-4.0	258	1.39
JENDL-5.0	199	1.06
JEFF-3.3	322	1.38
TENDL-2021	374	1.79
CENDL-3.2	211	0.97

3.2. Thermal Criticality Benchmarks

Table 5 presents the k_{eff} values calculated by McCARD for the 54 thermal benchmark problems, and Figure 5 shows the difference between the calculated and experimental k_{eff} . In the LEU-COMP-THERMAL cases, CENDL-3.2 showed lower results than the other ENDLs, whereas JEFF3.3 and TENDL-2021 showed relatively higher results. Table 6 shows the RMS errors and chi square values for the thermal benchmark problems. When excluding the PU-SOL-THERMAL cases, there were no significant differences in k_{eff} among the different ENDLs in the thermal benchmark cases. In the PU-SOL-THERML cases, the difference in k_{eff} ranged from -1327 pcm to 2220 pcm. In all thermal cases, RMS errors ranged from 252 pcm to 512 pcm, while the chi square values were from 0.72 to 1.24. In the 54 thermal benchmarks, the average uncertainty of k_{exp} is about 297 pcm. However, for the thermal benchmarks excluding PU-SOL-THERMAL, RMS errors ranged from 180 pcm to 272 pcm and chi square values were from 0.63 to 0.96.

Table 5. k_{eff} values for the thermal benchmarks with the different evaluated nuclear data libraries.

No.	Short Name	k_{eff} (McCARD) *						
		ENDF/B-VII.1	ENDF/B-VIII.0	JENDL-4.0	JENDL-5.0	JEFF-3.3	TENDL-2021	CENDL-3.2
32	ORNL-1	0.99772	0.99785	0.99889	0.99761	0.99634	0.99680	0.99656
33	ORNL-2	0.99679	0.99712	0.99851	0.99723	0.99577	0.99652	0.99587
34	ORNL-3	0.99329	0.99370	0.99487	0.99357	0.99256	0.99320	0.99209
35	ORNL-4	0.99483	0.99535	0.99648	0.99565	0.99408	0.99490	0.99370
36	ORNL-10	0.99883	0.99844	0.99846	0.99780	0.99695	0.99793	0.99734
37	LCT-001 c1	1.00013	0.99996	1.00063	0.99996	0.99980	1.00102	0.99786
38	LCT-001 c2	0.99941	0.99914	0.99997	0.99872	0.99899	0.99988	0.99706
39	LCT-001 c3	0.99903	0.99850	0.99869	0.99877	0.99878	1.00013	0.99675
40	LCT-001 c4	0.99970	0.99931	1.00030	0.99924	1.00025	1.00067	0.99721
41	LCT-001 c5	0.99763	0.99715	0.99803	0.99715	0.99775	0.99870	0.99538
42	LCT-001 c6	0.99958	0.99926	0.99925	0.99938	0.99946	1.00044	0.99770
43	LCT-001 c7	0.99907	0.99857	0.99910	0.99896	0.99874	0.99977	0.99650
44	LCT-001 c8	0.99774	0.99749	0.99736	0.99792	0.99704	0.99929	0.99585
45	LCT-002 c1	0.99907	0.99767	0.99962	0.99911	0.99942	0.99919	0.99730
46	LCT-002 c2	1.00038	0.99899	1.00060	1.00059	1.00083	1.00021	0.99868
47	LCT-002 c3	0.99993	0.99857	1.00010	0.99968	1.00024	0.99962	0.99832
48	LCT-006 c1	1.00015	0.99960	1.00115	0.99929	1.00191	1.00216	0.99872
49	LCT-006 c2	1.00079	0.99995	1.00144	1.00016	1.00188	1.00286	0.99884
50	LCT-006 c3	1.00055	0.99971	1.00132	0.99983	1.00212	1.00274	0.99880
51	LCT-006 c4	1.00027	0.99980	1.00098	0.99988	1.00140	1.00203	0.99862
52	LCT-006 c5	1.00021	0.99954	1.00093	0.99944	1.00133	1.00213	0.99809
53	LCT-006 c6	1.00051	1.00001	1.00144	0.99991	1.00209	1.00245	0.99880
54	LCT-006 c7	1.00046	0.99983	1.00105	0.99976	1.00170	1.00204	0.99868
55	LCT-006 c8	1.00027	0.99987	1.00108	0.99966	1.00119	1.00247	0.99884
56	LCT-006 c9	1.00039	0.99999	1.00112	1.00014	1.00105	1.00190	0.99817
57	LCT-006 c10	1.00032	0.99999	1.00083	0.99979	1.00084	1.00109	0.99797
58	LCT-006 c11	1.00031	0.99994	1.00101	1.00001	1.00135	1.00186	0.99790
59	LCT-006 c12	0.99993	0.99981	1.00078	0.99961	1.00109	1.00169	0.99794
60	LCT-006 c13	1.00009	0.99946	1.00054	0.99969	1.00065	1.00104	0.99792
61	LCT-006 c14	1.00039	1.00019	1.00097	1.00015	1.00040	1.00093	0.99835
62	LCT-006 c15	1.00025	0.99988	1.00076	0.99994	1.00073	1.00089	0.99781
63	LCT-006 c16	1.00015	0.99987	1.00087	1.00006	1.00050	1.00098	0.99805
64	LCT-006 c17	1.00014	0.99966	1.00051	1.00027	1.00044	1.00055	0.99805
65	LCT-006 c18	1.00013	0.99962	1.00066	0.99970	1.00034	1.00121	0.99791
66	LCT-010 c9	1.00020	0.99921	1.00122	1.00043	1.00038	1.00034	0.99882
67	LCT-010 c11	1.00091	0.99952	1.00121	1.00070	1.00077	1.00134	0.99951
68	LCT-010 c12	1.00012	0.99861	1.00050	1.00018	0.99991	0.99953	0.99840
69	LCT-010 c14	1.00189	1.00025	1.00228	1.00126	1.00366	1.00362	1.00060
70	LCT-010 c15	1.00267	1.00086	1.00286	1.00139	1.00391	1.00393	1.00131
71	LCT-010 c16	1.00306	1.00134	1.00347	1.00231	1.00469	1.00354	1.00161
72	LCT-010 c17	1.00255	1.00069	1.00293	1.00216	1.00405	1.00367	1.00168
73	LCT-010 c18	1.00249	1.00049	1.00306	1.00179	1.00392	1.00352	1.00109
74	LCT-017 c13	0.99924	0.99831	0.99855	0.99854	0.99890	0.99931	0.99700
75	LCT-017 c15	0.99790	0.99745	0.99782	0.99797	0.99908	0.99882	0.99695
76	LCT-017 c18	0.99938	0.99830	0.99917	0.99858	1.00001	1.00022	0.99819
77	LCT-017 c21	0.99890	0.99760	0.99881	0.99824	0.99942	0.99986	0.99732
78	IPEN/MB-01	1.00302	1.00220	1.00146	1.00289	1.00268	1.00289	1.00080
79	LMT-007 c1	1.00005	0.99768	0.99909	0.99775	1.00097	1.00032	0.99699
80	LMT-007 c2	0.99939	0.99776	0.99899	0.99884	1.00027	0.99945	0.99705
81	PNL-3	0.99371	0.98738	0.99426	0.98745	0.98857	0.98690	1.00470
82	PNL-4	0.99953	0.99315	1.00073	0.99197	0.99484	0.99278	1.01131
83	PNL-5	1.00569	0.99961	1.00799	0.99956	1.00128	0.99996	1.01956
84	PST011c16-1	1.00903	1.00312	1.01202	1.00320	1.00479	1.00275	1.02270
85	ORNL-11	1.00120	0.99968	0.99624	1.00281	1.00135	1.00007	0.99956

* Statistical uncertainties of the calculated k_{eff} are less than 10 pcm.

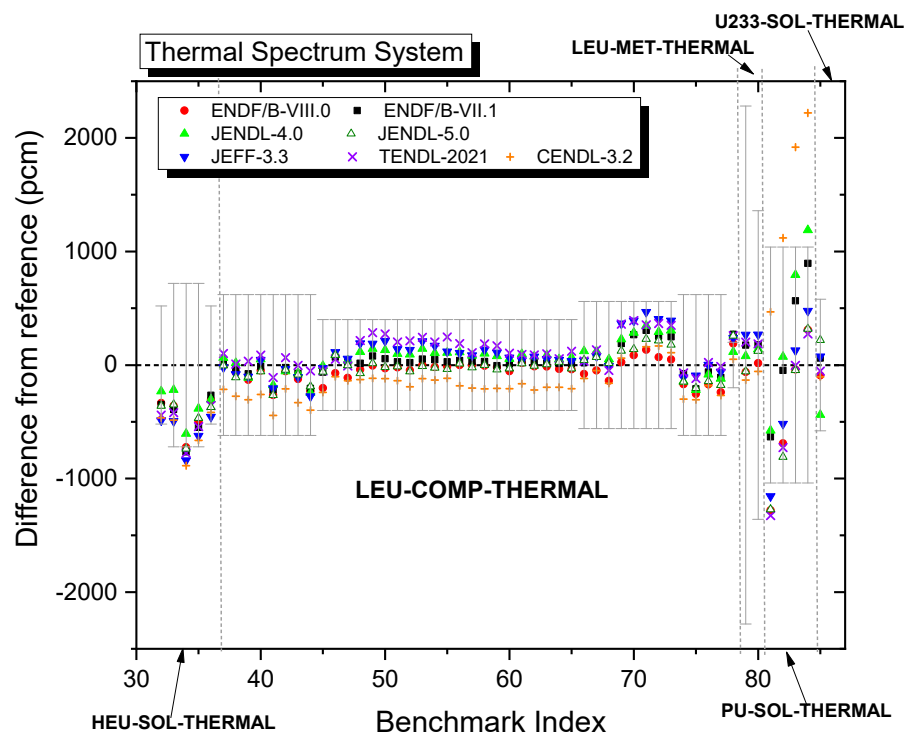


Figure 5. The difference between calculated and experimental k_{eff} by ENDL for the ICSBEP thermal benchmarks.

Table 6. RMS errors and chi square values of the 54 thermal benchmarks for different evaluated nuclear data libraries.

ENDL	All Cases		Cases Excluding PU-SOL-THERMAL		PU-SOL-THERMAL	
	RMS Error (pcm)	χ^2	RMS Error (pcm)	χ^2	RMS Error (pcm)	χ^2
ENDF/B-VII.1	252	0.76	195	0.71	620	1.19
ENDF/B-VIII.0	265	0.72	180	0.63	735	1.43
JENDL-4.0	279	0.77	190	0.68	777	1.48
JENDL-5.0	274	0.77	186	0.69	762	1.48
JEFF-3.3	308	0.96	257	0.93	674	1.31
TENDL-2021	311	0.99	241	0.95	760	1.48
CENDL-3.2	512	1.24	272	0.96	1619	3.05

Regarding these results, it can be observed that there are no significant differences in k_{eff} between the new and old version ENDLs. The RMS error of ENDF/B-VII.1 is 252 pcm whereas that of ENDF/B-VIII.0 is 265 pcm. Similarly, the RMS error of JENDL-4.0 is 279 pcm while that of JENDL-5.0 is 274 pcm. In the same manner as the fast benchmark cases, the JEFF-3.3 results are very similar to the TENDL-2021 results; the RMS errors of JEFF-3.3 and TENDL-2021 are 308 pcm and 311 pcm, respectively. In the PU-SOL-THERMAL cases, there is wide disparity in k_{eff} among the ENDLs as shown in Figure 5 and Table 6. It is worth mentioning that the difference in the thermal ^{239}Pu cross sections among the ENDLs affects the k_{eff} in the thermal spectrum system with fuels containing a significant fraction of plutonium.

3.3. Code-to-Code Comparison for ICSBEP Benchmarks

For code verification and validation, the McCARD results were compared to the MCNP results obtained from References [2,13] for the selected ICSBEP benchmark problems. Figure 6 shows the difference between k_{eff} values by the McCARD and MCNP calculations, and Table 7 summarizes the k_{eff} differences between the two codes for each benchmark category as RMS differences. The difference ($\Delta\rho_{MCNP}$) in k_{eff} between the McCARD and MCNP codes was calculated by

$$\Delta\rho_{MCNP} = \frac{k_{McCARD} - k_{MCNP}}{k_{McCARD} \cdot k_{MCNP}} \cdot 10^5. \quad (4)$$

where k_{McCARD} and k_{MCNP} are the k_{eff} by the McCARD and MCNP codes, respectively. In the fast benchmark cases, the RMS difference for ENDF/B-VII.1 was 26 pcm whereas those for ENDF/B-VIII.0 and JENDL-4.0 were 29 and 28 pcm, respectively. In the thermal benchmark cases, the RMS difference for ENDF/B-VII.1 was 53 pcm, while those for ENDF/B-VIII.0 and JENDL-4.0 were both 45 pcm. In the NJOY processing, the thermal scattering cross sections are sensitively affected by the thermal scattering law parameters, which are used in the LEAPR module. Accordingly, the difference between the thermal scattering cross sections used in the McCARD and MCNP calculations may have led to the increased RMS difference in the thermal benchmarks. In all benchmark cases, the RMS differences ranged from 40 pcm to 49 pcm. Considering that the statistical uncertainties of the MCNP results were less than 100 pcm, it was concluded that the k_{eff} results between McCARD and MCNP are in excellent agreement.

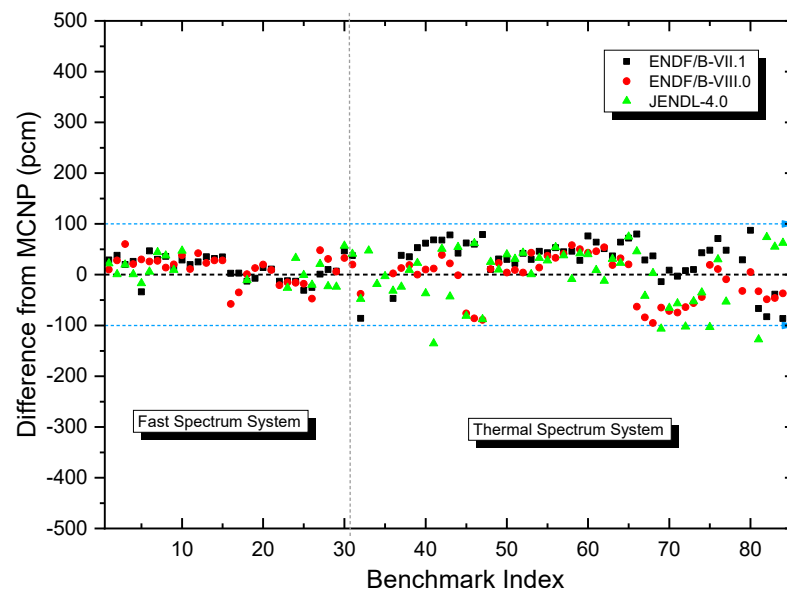


Figure 6. The difference between k_{eff} values by McCARD and MCNP calculations for the selected ICSBEP benchmark problems.

Table 7. The RMS difference between k_{eff} results by McCARD and MCNP calculations.

ENDL	RMS Difference in k_{eff} (pcm)		
	FAST	THERMAL	Total
ENDF/B-VII.1	26	53	45
ENDF/B-VIII.0	29	45	40
JENDL-4.0	28	45	49

4. Uncertainty Analyses of Criticality in ICSBEP Benchmarks

4.1. Uncertainty of k_{eff} Due to Uncertainty of Cross Sections

This section was prepared to provide an understanding of the difference in k_{eff} among the ENDLs with their cross section covariance data. In general, the mean of MC estimates on a criticality (i.e., k_{eff}) and its variance can be expressed by

$$\overline{k_{eff}} = \lim_{N \rightarrow \infty} \frac{1}{N} \sum_{i=1}^N k_{eff}^i \quad (5)$$

$$\sigma^2[k_{eff}] = \lim_{N \rightarrow \infty} \frac{1}{N} \sum_{i=1}^N (k_{eff}^i - \overline{k_{eff}})^2 \quad (6)$$

If one assumes that the total uncertainty on k_{eff} comes from statistical uncertainties of MC calculations and cross section uncertainties by their covariance data, Equation (6) can be rewritten as

$$\sigma^2[k_{eff}] = \lim_{N \rightarrow \infty} \frac{1}{N} \sum_{i=1}^N (k_{eff}^i - \langle k_{eff}^i \rangle + \langle k_{eff}^i \rangle - \overline{k_{eff}})^2 \quad (7)$$

The angular bracket in $\langle k_{eff} \rangle$ means the operator implying the expected value of a quantity on it. By the first-order Taylor expansion for $\langle k_{eff} \rangle$ about the mean values of nuclear reaction cross section, $\langle k_{eff}^i \rangle - \overline{k_{eff}}$ can be expressed by

$$\langle k_{eff}^i \rangle - \overline{k_{eff}} \approx \sum_i \sum_\alpha \sum_g \left((x_{\alpha,g}^i)_k - \overline{x_{\alpha,g}^i} \right) \left(\frac{\partial k_{eff}}{\partial x_{\alpha,g}^i} \right) \quad (8)$$

$x_{\alpha,g}^i$ is the α -type microscopic cross section of isotope i for energy group g . Substituting Equation (8) into Equation (7), one can obtain

$$\sigma^2(k_{eff}) = \sigma_S^2(k_{eff}) + \sigma_X^2(k_{eff}) \quad (9)$$

where

$$\sigma_S^2(k_{eff}) = \lim_{N \rightarrow \infty} \frac{1}{N} \sum_{i=1}^N (k_{eff}^i - \langle k_{eff}^i \rangle)^2 \quad (10)$$

$$\begin{aligned} \sigma_X^2(k_{eff}) &= \lim_{N \rightarrow \infty} \frac{1}{N} \sum_{j=1}^N (\langle k_{eff}^j \rangle - \overline{k_{eff}})^2 \\ &= \sum_{i,\alpha,g} \sum_{i',\alpha',g'} \text{cov}[x_{\alpha,g}^i, x_{\alpha',g'}^{i'}] \left(\frac{\partial k_{eff}}{\partial x_{\alpha,g}^i} \right) \left(\frac{\partial k_{eff}}{\partial x_{\alpha',g'}^{i'}} \right) \end{aligned} \quad (11)$$

$\sigma_S^2(k_{eff})$ is the statistical contribution on the variance of k_{eff} whereas $\sigma_X^2(k_{eff})$ is commonly known as the sandwich equation for S/U analyses. $\text{cov}[x_{\alpha,g}^i, x_{\alpha',g'}^{i'}]$ is the cross section covariance matrix from each ENDL. The sensitivity coefficients can be calculated by the MC perturbation technique. This S/U analysis capability was already implemented in the McCARD code [19].

To examine the uncertainty in k_{eff} due to the uncertainties of the cross sections, the benchmark problems, which have the largest difference in k_{eff} among ENDLs, were selected for each category. According to it, the uncertainty quantification in k_{eff} for Jezebel-240, Flattop-25, LCT-006c1, and PNL-5 were performed with the covariance data in each ENDL. ENDF/B-VII.1, ENDF/B-VIII.0, JENDL-4.0, JENDL-5.0, JEFF-3.3, and TENDL-2021 provide the covariance data for ν and cross section on the MF31 and MF33 sections in each ENDL, whereas there is no covariance data in the CENDL-3.2.

Table 8 shows the error of k_{eff} from reference and the uncertainty in k_{eff} due to the uncertainty of cross sections ($=\sigma_X^2(k_{eff})$) for each ENDLs by the McCARD S/U calculations. The standard deviations of the errors among ENDLs are 194 pcm, 265 pcm, 121 pcm, and 358 pcm for Jezebel-240, Flattop-25, LCT-006 c1, PNL-5 benchmarks, respectively. Overall, it is noted that the errors of k_{eff} are less than the uncertainties of k_{eff} by the covariance data from each ENDL except the PNL-5 case with JENDL-4.0. Regarding the results, it was observed that the cross section data used in the four benchmarks have instability or uncertainty, and this led to the error of k_{eff} from the reference.

Table 8. Error of k_{eff} from reference and uncertainty of k_{eff} due to the uncertainty of cross sections for the four ICSBEP benchmarks.

ENDL	Jezebel-240		Flattop-25		LCT-006 c1		PNL-5	
	Error from Ref. *	Unc. from Cov. **	Error from Ref. *	Unc. from Cov. **	Error from Ref. *	Unc. from Cov. **	Error from Ref. *	Unc. from Cov. **
ENDF/B-VII.1	41	616	298	1456	15	904	566	624
ENDF/B-VIII.0	160	966	107	1134	−40	529	−39	1146
JENDL-4.0	−151	523	−188	848	115	919	793	510
JENDL-5.0	−130	684	81	879	−71	435	−44	1110
JEFF-3.3	151	906	431	1217	191	685	128	737
TENDL-2021	360	400	541	1222	216	683	−4	730
Standard Deviation (Error from Ref.)	194	-	265	-	121	-	358	-

* Error of k_{eff} from Reference (pcm). ** Uncertainty of k_{eff} due to the uncertainty of cross sections (pcm) $=\sigma_X^2(k_{eff})$.

Meanwhile, O. Cabellos et al. presented the uncertainties of k_{eff} from the covariance data of various ENDLs by NDaST in the ICSBEP benchmark suite [20]. In the HEU category, the averaged uncertainties in k_{eff} due to the ^{235}U covariance data for ENDF/B-VIII.0, JENDL-3.3T4, ENDF/B-VIII.1, and JENDL-4.0 were 1012 pcm, 1190 pcm, 1345 pcm, and 679 pcm, whereas the averaged uncertainties of k_{eff} due to the ^{239}Pu covariance data in the PU-SOL-THERM category were 1157 pcm, 967 pcm, 608 pcm, and 687 pcm. It was noted that they were very similar to the uncertainties of the Flattop-25 in the HEU category and the PNL-3 in the PU-SOL-THERM category by the McCARD code.

4.2. Quantitative Analysis for Group-Wise Reactivity

This section shows the results of the quantitative analyses for the reactivity differences between ENDF/B-VII.1 and the other ENDL. In the quantitative analysis, the differences in absorption and fission cross sections between ENDF/B-VII.1 and the other ENDL can be expressed by the reactivity differences in the “pcm” unit for each energy group. The reactivity differences due to the difference of the absorption and fission cross section between ENDF/B-VII.1 and the other ENDL can be calculated by

$$\Delta\rho_{a,g}^i = \left[\frac{1}{(k_\infty)_{E71}} - \frac{\sum_{g',k'} N^{k'} \phi_{g'}(x_{a,g'}^{k'})_{E71} - N^i \phi_g((x_{a,g}^i)_{E71} - (x_{a,g}^i)_{OTR})}{\sum_{g',k'} N^{k'} \phi_{g'}(v x_{f,g'}^{k'})_{E71}} \right], \quad (12)$$

$$\Delta\rho_{f,g}^i = \left[\frac{1}{(k_\infty)_{E71}} - \frac{\sum_{g',k'} N^{k'} \phi_{g'}(x_{a,g'}^{k'})_{E71}}{\sum_{g',k'} N^{k'} \phi_{g'}(v x_{f,g'}^{k'})_{E71} - N^i \phi_g((v x_{f,g}^i)_{E71} - (v x_{f,g}^i)_{OTR})} \right], \quad (13)$$

where

$$(k_{\infty})_{E71} = \frac{\sum_{g',k'} N^{k'} \phi_{g'} (\nu x_{f,g'}^{k'})_{E71}}{\sum_{g',k'} N^{k'} \phi_{g'} (x_{a,g'}^{k'})_{E71}}$$

$(x_{a,g}^i)_{E71}$ and $(x_{a,g}^i)_{OTR}$ means the ENDF/B-VII.1 and the other ENDL absorption cross section of isotope i for energy group g . $(\nu x_{f,g}^i)_{E71}$ and $(\nu x_{f,g}^i)_{OTR}$ are the product of the number of neutrons by a fission (ν) and the g -th group fission cross section of isotope i for ENDF/B-VII.1 and the other ENDL, respectively. The reactivity difference indicates the contribution of the difference in the cross section to the error in reactivity or criticality [21].

Figures 7 and 8 show the reactivity difference due to the difference of ^{239}Pu absorption and fission cross sections between ENDF/B-VII.1 and the other ENDLs for the PNL-5 benchmarks. The group-wise reactivity analyses due to the ^{239}Pu cross section changes were conducted out because ^{239}Pu is a major fuel isotope in the PNL-5 benchmark. The reactivity difference ($\Delta\rho_{E71}$) between ENDF/B-VII.1 and the other ENDL was calculated by

$$\Delta\rho_{E71} = \frac{k_{OTR} - k_{E71}}{k_{OTR} \cdot k_{E71}} \cdot 10^5. \quad (14)$$

k_{E71} and k_{OTR} are the k_{eff} by ENDF/B-VII.1 and the other ENDL. Table 9 presents the sum of group-wise reactivity differences due to the ^{239}Pu cross section changes. There are considerable reactivity differences due to the changes of ^{239}Pu absorption and fission cross sections at the thermal energy ranges (10^{-3} – 1 eV). The individual group reactivity differences ranged from -1000 pcm to 900 pcm, but the group-wise reactivity differences due to absorption and fission cross section changes have the opposite sign. Therefore, the effects on the absorption and fission cross section changes were canceled out each other. It is observed that the sum of the reactivity changes by ^{239}Pu cross sections ranged from -259 pcm to 288 pcm. Meanwhile, the total reactivity difference ranged from -1353 pcm to 610 pcm because the leakage effects and the reactivity changes by the other nuclides (^{240}Pu , ^1H , ^{16}O , Fe, Ni, Cr) were considered in these total reactivity analyses. In the PNL-5 criticality analyses, the k_{eff} of ENDF/B-VIII.0, JENDL-5.0, JEFF-3.3, TENDL-2021 were less than ENDF/B-VII.1 whereas those of JENDL-4.0 and CENDL-3.2 were larger than ENDF/B-VII.1.

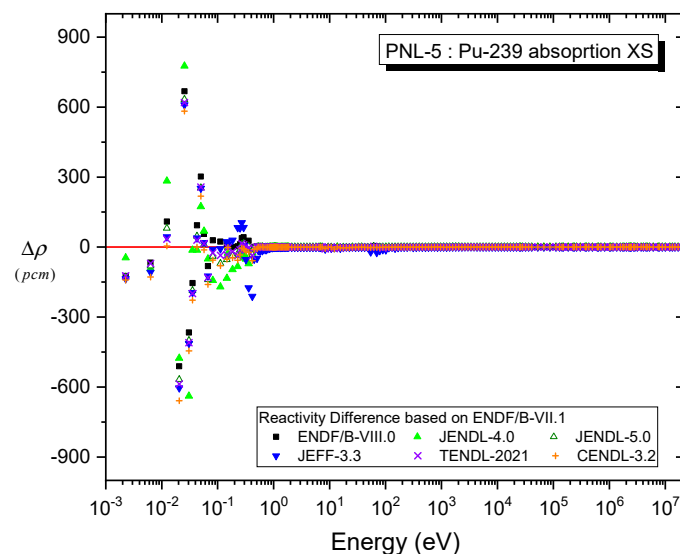


Figure 7. The reactivity difference due to the difference of ^{239}Pu absorption cross sections between ENDF/B-VII.1 and the other ENDL for PNL-5.

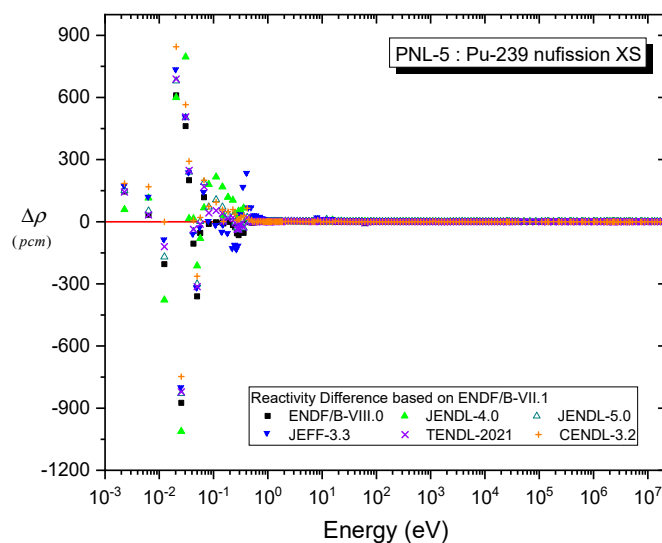


Figure 8. The reactivity difference due to the difference of ^{239}Pu fission cross sections between ENDF/B-VII.1 and the other ENDL for PNL-5.

Table 9. The sum of group-wise reactivity difference due to the difference of ^{239}Pu fission cross sections between ENDF/B-VII.1 and the other ENDLs for PNL-5.

ENDL	k_{eff}	$\Delta\rho_{E71}$ (pcm) *	Sum of Group-Wise Reactivity Differences (pcm)		
			^{239}Pu Absorption	^{239}Pu Fission	^{239}Pu Total
ENDF/B-VII.1	1.00569	-	-	-	-
ENDF/B-VIII.0	0.99961	-605	98	-266	-168
JENDL-4.0	1.00799	227	-1071	1163	92
JENDL-5.0	0.99956	-610	-873	816	-57
JEFF-3.3	1.00128	-438	-1084	796	-288
TENDL-2021	0.99996	-570	-910	701	-209
CENDL-3.2	1.01956	1353	-1642	1900	259

* $\Delta\rho_{E71}$ is the total reactivity difference between ENDF/B-VII.1 and the other ENDLs.

5. Conclusions

In this study, ICSBEP criticality analyses were conducted using the McCARD code for 85 selected benchmark problems with seven evaluated nuclear data libraries (ENDLs): ENDF/B-VII.1, ENDF/B-VIII.0, JENDL-4.0, JENDL-5.0, JEFF-3.3, TENDL-2021, and CENDL-3.2. To prepare some of the up-to-date ENDLs (i.e., ENDF/B-VIII.0, JENDL-5.0, JEFF-3.3, CENDL-3.2) for McCARD calculations, continuous energy nuclear data libraries in ACE format were generated by the NJOY code. Regarding the criticality analyses, it was noted that the k_{eff} results were sensitive to the ENDL. It is worth mentioning that the new version ENDLs showed better performance in the fast benchmark cases, while there were no significant differences in k_{eff} among the different ENDLs in the thermal benchmark cases. In all benchmark cases, the TENDL-2021 results were very similar to the JEFF-3.3 results because TENDL-2021 shared the raw nuclear data of the JEFF ENDL for $^1,^2,^3\text{H}$, $^3,^4\text{He}$, $^6,^7\text{Li}$, $^{10,11}\text{B}$, $^7,^9\text{Be}$, $^{12,13}\text{C}$, $^{14,15}\text{N}$, $^{16,17,18}\text{O}$, ^{19}F , ^{232}Th , $^{233,235,238}\text{U}$ and ^{239}Pu isotopes.

The sensitivity of the k_{eff} results to the different ENDLs may impact certain nuclear core design parameters such as shutdown margin, critical boron concentration, and power defects. Consequently, nuclear core designers should consider this sensitivity to the ENDL as a margin of uncertainty. This study and k_{eff} results will be a good reference for the development of new types of nuclear cores or new design codes.

Author Contributions: Conceptualization, H.J.P.; methodology, H.J.P.; software, H.J.P. and S.H.C.; validation, H.J.P., M.A., S.H.C. and S.-A.Y.; formal analysis, H.J.P. and S.-A.Y.; investigation, H.J.P.; resources, H.J.P.; data curation, H.J.P.; writing—original draft preparation, H.J.P.; writing—review and editing, S.H.C.; visualization, H.J.P.; supervision, H.J.P.; project administration, S.H.C.; funding acquisition, H.J. and S.H.C. All authors have read and agreed to the published version of the manuscript.

Funding: This research was supported by KAERI and King Abdullah City for Atomic and Renewable Energy (K.A.CARE), Kingdom of Saudi Arabia, within the Joint Research and Development Center.

Conflicts of Interest: The authors declare no conflict of interest. The funders had no role in the design of the study; in the collection, analyses, or interpretation of data; in the writing of the manuscript, or in the decision to publish the results.

Abbreviations

ENDL	Evaluated Nuclear Data Library
JAERI	Japan Atomic Energy Research Institute
JENDL	Japanese Evaluated Nuclear Data Library
JEFF	Joint Evaluated Fission and Fusion
CENDL	Chinese general purpose Evaluated Nuclear Data Library
ICSBEP	International Criticality Safety Benchmark Problem
RMS	Root Mean Square
LEU	Low-Enriched Uranium
HEU	High-Enriched Uranium
MET	Metal
COMP	Compound
SOL	Solution
TSL	Thermal Scattering Law

References

- Chadwick, M.B.; Herman, M.; Obložinský, P.; Dunn, M.; Danon, Y.; Kahler, A.; Smith, D.; Pritychenko, B.; Arbanas, G.; Arcilla, R.; et al. ENDF/B-VII.1 Nuclear Data for Science and Technology: Cross Sections, Covariances, Fission Product Yields and Decay Data. *Nucl. Data Sheets* **2011**, *112*, 2887–2996. [[CrossRef](#)]
- Brown, D.A.; Chadwick, M.B.; Capote, R.; Kahler, A.C.; Trkov, A.; Herman, M.W.; Sonzogni, A.A.; Danon, Y.; Carlson, A.D.; Dunn, M.; et al. ENDF/B-VIII.0: The 8th Major Release of the Nuclear Reaction Data Library with CIELO-project Cross Sections, New Standards and Thermal Scattering Data. *Nucl. Data Sheets* **2018**, *148*, 1–142. [[CrossRef](#)]
- Shibata, K.; Iwamoto, O.; Nakagawa, T.; Iwamoto, N.; Ichihara, A.; Kunieda, S.; Chiba, S.; Furutaka, K.; Otuka, N.; Ohsawa, T.; et al. JENDL-4.0: A New Library for Nuclear Science and Engineering. *J. Nucl. Sci. Technol.* **2011**, *48*, 1–30. [[CrossRef](#)]
- Iwamoto, O.; Iwamoto, N.; Shibata, K.; Ichihara, A.; Kunieda, S.; Minato, F.; Nakayama, S. Status of JENDL. *EPJ Web Conf.* **2020**, *239*, 09002. [[CrossRef](#)]
- Plompen, A.J.M.; Cabellos, O.; Jean, C.D.S.; Fleming, M.; Algora, A.; Angelone, M.; Archier, P.; Bauge, E.; Bersillon, O.; Blokhin, A.; et al. The Joint Evaluated Fission and Fusion Nuclear Data Library, JEFF-3.3. *Eur. Phys. J. A* **2020**, *56*, 181. [[CrossRef](#)]
- Koning, A.J.; Rochman, D.; Sublet, J.-C.; Dzysiuk, N.; Fleming, M.; van der Marck, S. TENDL: Complete Nuclear Data Library for Innovative Nuclear Science and Technology. *Nucl. Data Sheets* **2019**, *155*, 1–55. [[CrossRef](#)]
- Koning, A.J.; Duijvestijn, M.C.; Hilaire, S. TALYS-1.0. In Proceedings of the International Conference on Nuclear Data for Science and Technology, Nice, France, 22–27 April 2007; Volume 211.
- Ge, Z.; Xu, R.; Wu, H.; Zhang, Y.; Chen, G.; Jin, Y.; Shu, N.; Chen, Y.; Tao, X.; Tian, Y.; et al. CENDL-3.2: The New Version of Chinese General Purpose Evaluated Nuclear Data Library. *EPJ Web Conf.* **2020**, *239*, 09001. [[CrossRef](#)]
- International Handbook of Evaluated Criticality Safety Benchmark Experiments*; OECD Nuclear Energy Agency Report NEA/NSC/DOC(95)03; OECD Nuclear Energy Agency: Paris, France, 1998.
- Greene, N.M.; Petrie, L.M.; Westfall, R.M.; Bucholz, J.A.; Hermann, O.W.; Fraley, S.K. SCALE: A Modular Code System for Performing Standardized Computer Analyses for Licensing Evaluations; ORNL/TM-2005/39; U.S. Nuclear Regulatory Commission: Washington, DC, USA, 2005.
- MCNP. *User Manual—Code Version 6.2*; LA-UR-17-29981; Los Alamos National Security LLC: Los Alamos, MN, USA, 2017.
- Alcouffe, R.E.; Baker, R.S.; Brinkley, F.W.; Marr, D.R.; O'Dell, R.D.; Walters, W.F. DANTSYS: A Diffusion Accelerated Neutron Particle Transport Code System; LA-12969-M; Los Alamos National Lab.: Los Alamos, NM, USA, 1995.
- van der Marck, S.C. Benchmarking ENDF/B-VII.1, JENDL-4.0, and JEFF-3.1.1 with MCNP6. *Nucl. Data Sheets* **2012**, *113*, 2935–3005. [[CrossRef](#)]

14. Park, H.J.; Kang, H.; Lee, H.C.; Cho, J.Y. Comparison of ENDF/B-VIII.0 and ENDF/B-VII.1 in Criticality, Depletion Benchmark, and Uncertainty Analyses by McCARD. *Ann. Nucl. Energy* **2019**, *131*, 443–459. [[CrossRef](#)]
15. Zheng, L.; Huang, S.; Wang, K. Criticality Benchmarking of ENDF/B-VIII.0 and JEFF-3.3 Neutron Data Libraries with RMC code. *Nucl. Eng. Technol.* **2020**, *52*, 1917–1925. [[CrossRef](#)]
16. Kim, K.-S.; Wieselquist, W.A. Neutronic Characteristics of ENDF/B-VIII.0 Compared to ENDF/B-VII.1 for Light-Water Reactor Analysis. *J. Nucl. Eng.* **2021**, *2*, 318–335. [[CrossRef](#)]
17. Shim, H.J.; Han, B.-S.; Jung, J.-S.; Park, H.-J.; Kim, C.-H. McCARD: Monte Carlo Code for Advanced Reactor Design and Analysis. *Nucl. Eng. Technol.* **2012**, *44*, 161–176. [[CrossRef](#)]
18. MacFarlane, R.E.; Muir, D.W.; Boicourt, R.M.; Kahler, A.C., III; Conlin, J.L. *The NJOY Nuclear Data Processing System Version 2016*; LA-UR-17-20093; Los Alamos National Lab.: Los Alamos, NM, USA, 2016.
19. Park, H.J.; Shim, H.J.; Kim, C.H. Uncertainty Propagation in Monte Carlo Depletion Analysis. *Nucl. Sci. Eng.* **2011**, *167*, 196–208. [[CrossRef](#)]
20. Cabellos, O.; Dyrda, J.; Soppera, N. Checking, Processing and Verification of Nuclear Data Covariances. *EPJ Nucl. Sci. Technol.* **2018**, *4*, 39. [[CrossRef](#)]
21. Park, H.J.; Shim, H.J.; Joo, H.G.; Kim, C.H. Generation of Few-group Diffusion Theory Constants by Monte Carlo Code McCARD. *Nucl. Sci. Eng.* **2012**, *172*, 66–77. [[CrossRef](#)]